EVS30 Symposium
Stuttgart, Germany, October 9 - 11, 2017

Capacity Recovery Effect in Lithium Sulphur Batteries for Electric Vehicles

Christian Maurer[1], Walter Commerell[1], Andreas Hintennach[2], Andreas Jossen[3]
[1]*Hochschule Ulm (HS Ulm), Prittwitzstr. 10, 89075 Ulm, Germany, c.maurer@hs-ulm.de*
[2]*Daimler AG, HPC G012, Hanns-Klemm-Str. 45, 71034 Böblingen, Germany, andreas.hintennach@daimler.com*
[3]*Technische Universität München (TUM), Arcisstr. 21, 80333 Munich, Germany, andreas.jossen@tum.de*

Abstract

Lithium sulphur batteries have a promisingly high theoretical specific energy density of about 2600 Wh/kg and an expected practical specific energy density of about 500-600 Wh/kg. Therefore, it is a highly promising future energy storage technology for electric vehicles. Beside these advantages, this technology shows a low cell capacity at high discharge currents. Due to the capacity recovery effect up to 20% of the total cell capacity become available again with some rest time. This study shows a newly developed capacity recovery model for lithium sulphur batteries. Due to long rest periods of electric vehicles, this effect has important influence on the usable cell capacity and depth of discharge in lithium sulphur batteries.

Keywords: battery, discharge rate, energy recovery, lithium battery, modeling

1 Introduction

Lithium sulphur batteries (LiS) are a highly promising future energy storage technology for electric vehicles, due to the very high theoretical specific energy density of about 2600 Wh/kg. One reason therefore is the high specific capacity of 1675 Ah/kg of the sulphur cathode. The theoretical specific energy density is five times higher than state of the art lithium-ion technologies and the expected practical specific energy density is about 500-600 Wh/kg [1].
Furthermore, the potential of low manufacturing costs due to less expensive cathode materials increases their value even more. In state of the art lithium nickel manganese cobalt oxide cells the cathode comes up with 24% of the total cell costs [2].
Despite these strong advantages, the LiS technology faces some challenges before it can be used in real applications. To start with, the LiS technology has a high degradation rate. The high specific densities can only be reached in the first few full cycles of this technology. After 50 to 200 full cycles the usable cell capacity is less than 80% of its initial cell capacity [3]. A key mechanism of this capacity loss is the huge dilatation of the cell. One reason for this dilatation is a volume change factor of 1.79 from pure sulphur educt S_8 to the lithium sulphur product Li_2S [4].
Another challenge is the multiple redox reactions in LiS batteries compared to lithium ion batteries. The reactivity and reaction kinetics decrease with increasing depth of discharge (DOD) [5]. The redox reactions consist of decreasing polysulfide chains which precipitate in the final lithium polysulfide Li_2S product. Equation 1 shows the overall redox reaction and equation 2 the simplified assumed multiple redox reaction equations [5].

$$16Li + S_8 \rightarrow 8Li_2S \tag{1}$$

$$
\begin{aligned}
S_8 + 2Li^+ + 2e^- &\rightarrow Li_2S_8 \\
Li_2S_8 + 2Li^+ + 2e^- &\rightarrow 2Li_2S_4 \\
Li_2S_4 + 2Li^+ + 2e^- &\rightarrow 2Li_2S_2 \\
Li_2S_4 + 6Li^+ + 6e^- &\rightarrow 4Li_2S
\end{aligned}
\tag{2}
$$

The main occurrences of these reaction products are presented in Fig.1 over DOD.

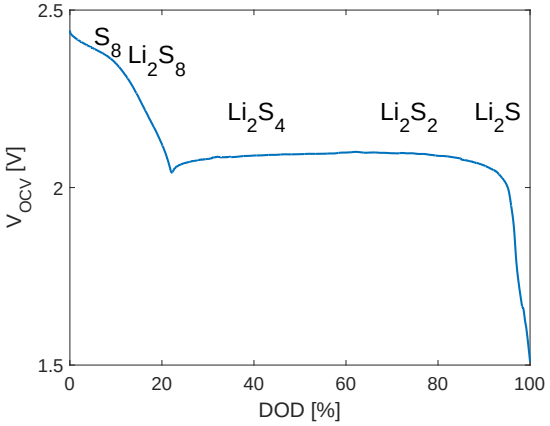

Figure 1: Open circuit voltage of a lithium sulphur cell with reaction products of the multiple reaction stages described in [5].

This open circuit voltage in Fig.1 consists of an upper or first voltage plateau, which ranges from 0% DOD to 22% DOD and a lower or second voltage plateau, which ranges from 22% DOD to 100% DOD as presented in Fig.1. Some LiS dependent mechanisms can be assigned to the specific plateaus. For instance, only in the first plateau a very high self-discharge rate is observed because of the shuttle effect [6] and [4]. In the second voltage plateau Li_2S is precipitated [5]. Only Li_2S is precipitated as a solid product in LiS cells as published in [7].

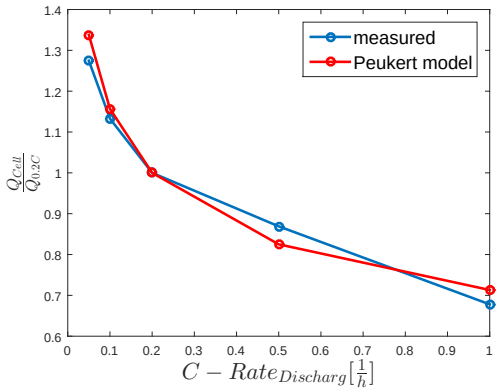

Figure 2: Relative cell capacity influenced by constant discharge current without rest time. The Peukert coefficient of the model is 1.2.

A further challenge for the LiS technology is the sulphur utilization. This utilization is bound to decrease with increasing discharge current. So the utilized sulphur influences the usable cell capacity as showed in Fig.2. Taking into account the constant discharge currents and the usable cell capacities, an empiric Peukert coefficient of 1.2 is calculated as shown in Fig.2.
The non utilized sulphur in the LiS technology shows the interesting effect, that parts of this non utilized sulphur become available during rest times. So this sulphur additional takes part at further discharging. The capacity due to this sulphur is considered as recovered capacity. This effect was published in [8] and [9].
However, very little is known about the influence of DOD with a variety of discharge currents on the recovered capacity. This study investigates the DOD dependent capacity recovery effect.

2 Capacity Recovery Effect

This section reflects the dynamic capacity recovery effect. A basic necessity for vehicular evaluations of the LiS technology are dynamical and utilizable models. In [10] a dynamical RC-model was published. A first mathematical model of LiS cells was published in [11]. In addition Marinescu et al. invented a simplified chemical model to describe the discharge and charge reaction mechanisms [12]. So far the recovery effect of a single DOD as an additional result of a self-discharge experiment was published in [9]. Also the recovery effect at a 100% DOD level was remarkable published in [8]. Our purpose of this work is the quantification of the recovering capacity of the cell and subsequently its veritable usage capacity. Additionally a dynamical capacity recovery model for LiS cells from a vehicular application point of view is developed. In vehicular applications rest times are not connected to specific DODs. In other words, the occurrence of recovery break times (t_{RBT}) for the recovery effect are DOD independent. In addition the recovered capacity is quite important to estimate the true usable cell capacity in LiS cells used in electric vehicles.
As described before the recovered capacity depends on sulphur utilization. We have described that the final product Li_2S of the reaction mechanism blocks sulphur and reaction products $Li_2S_x, 2 \geq x \geq 8$ in the carbon pores. These blocked products are one reason for the poor sulphur utilization and the huge difference between theoretical and practical cell capacity. Further, it is believed that the diffusion of dissolved polysulfides away from electrochemical active surfaces leads to low sulphur utilization [13]. So we assume that this Li_2S product diffuses with the time and unblocks active materials in some of the carbon matrix pores and we assume that dissolved polysulfides diffuse back to the active surface. This unblocking process is influenced by six parameters. First, the diffusion is bound to the initial diffusion rate of the cell. Second, the temperature influences the diffusion rate of the blocking Li_2S and diffusion of polysulfides. Third, the current history influences the precipitated structure of Li_2S. Fourth, t_{RBT} defines the amount of diffused Li_2S and diffused polysulfides. Fifth, the DOD determines the concentration of Li_2S. Sixth, the cell degradation determines the usable and available active material. To clarify, these parameters cannot be regarded solely. Moreover, there exist dependencies between these parameters. It is clear that this effect is relevant in vehicular applications.
The published time constant for the recovered capacity differ highly. On the one hand, a capacity recovery time constant between 18 to 24 minutes was published in [8]. In their study an Oxis 3.4Ah pouch cell was measured at a constant temperature of $30°C$ and the cell was discharged at 1C. The recovered capacity was measured after recovery break times t_{RBT} up to 4 hours at 100% DOD. On the other hand, in [9] a capacity recovery time constant of 50 hours was published. There a single 2.8Ah Sion Power pouch cell was used in a self-discharge experiment at 60% DOD and a constant temperature of $20°C$. The cell was discharged at C/9 and afterwards charged to 60% DOD. The recovered capacity after 24 hours of this cell was used to estimate the capacity recovery time constant. Despite, the different temperatures and different currents, these findings differ highly. So a separate first investigation is performed.

3 Experimental Capacity Recovery Study

In this section the experimental design of the capacity recovery study is described. We intend to examine the capacity recovery effect with respect to discharge current, DOD and recovery break time.

3.1 Recovery Time Constant

As noted above the published recovery time constants differ highly. So in this section we intend to analyse the recovery time constant in a first investigation. Therefore, we use a capacity recovery cycle, which consists of four cycles. The first cycle discharges and charges the cell at nominal 0.2C discharge and nominal 0.1C charge current. This cycle sets the cell in a reproducible condition. The second cycle discharges the cell at 0.8C discharge current for the recovery reference capacity and charges the cell at nominal 0.1C charge current. The third cycle is the same as the first. In the fourth cycle the cell is at first discharged at 0.8C discharge current, rests at a DOD of 100% for a t_{RBT} and discharges the cell a second time at 0.8C discharge current. The cumulated capacity of the first and the second discharge is the capacity of the fourth cycle, which consists of the constant current discharged capacity and the recovered capacity. Afterwards the cell is charged at nominal 0.1C charge current. This recovery cycle was repeated with a linear increasing t_{RBT} from 0 to 120 minutes. This first investigation is done in a climate chamber at a constant temperature of $25°C$. The recovered capacity was calculated using equation 3 by the subtraction of the cell capacity of the fourth cycle after its second discharge and the cell capacity of the second cycle. In order to estimate a recovery time constant the recovered capacity was modelled using equation 5. We illustrated the recovered capacities in Fig.3. Least-squares method calculated the gain factor k of 10.5% and the recovery time constant τ of 46 minutes used in equation 5 for this first investigation. This result is within the range of [8].

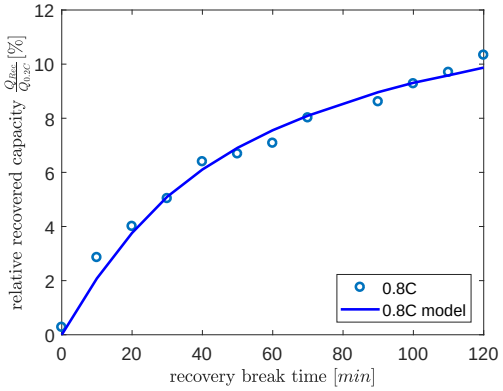

Figure 3: Measured and modelled recovered capacity after a 0.8C constant current discharge at 100% DOD and a recovery break time between 0 and 120 minutes at a constant temperature of $25°C$.

$$Q_{Rec} = Q_{4thCycle} - Q_{2ndCycle} \tag{3}$$

3.2 Recovery Cycle

The model proposed in this work, calculates the gained cell capacity due to the recovery effect and the t_{RBT}. Therefore, a DOD, current and t_{RBT} dependent function is evaluated (see equation 5).
In order to quantify the recovered capacity, we have chosen to set up a recovery cycle, which is quite similar to the described recovery cycle in section 3.1. On the contrary to the noted recovery cycle above the second and fourth cycle differ. The fixed discharge current at 0.8C in section 3.1 is replaced in this investigation by varied discharge currents. So the second cycle discharges the cell at a varied discharge current in order to get the reference capacity at the used discharge current and charges the cell at nominal 0.1C charge current. In the fourth cycle, the cell is at first discharged at the same varied discharge current as in the second cycle. At a specific DOD level a varied t_{RBT} is included. During this t_{RBT} capacity is recovered and extends the usable capacity of the cell. After this t_{RBT}, the cell is a second time discharged at the varied discharge current. Afterwards, the cell is charged again at nominal 0.1C charge current.
In order to reduce the cell degradation mentioned in section 1 and reach more comparable results, each cycle is limited by a maximal voltage of 2.35V and a minimal voltage of 1.7V. Furthermore, additives of the electrolyte are mainly decomposed at voltages near the limits as demonstrated in [14].
Therefore, the referenced cell capacity is also measured between these voltage limits at nominal 0.2C discharge current.
The experiment is done in a climate chamber at a constant temperature of $25°C$. The cells were cycled by a BaSyTec CTS with 32 channels.

3.3 Parameter Variation

Three parameters are varied in this capacity recovery study. The first parameter is t_{RBT}. Based on the feedback of the recovery time constant investigation (see Fig.3) four t_{RBT} were chosen. In order to get an applicable model, particular attention was paid to lower t_{RBT} with 15 min, 30 min 60 min and 120 min.
The second parameter, DOD was chosen to change in four equally spaced steps from 20 to 80 percent with respect to the defined upper and lower voltage limits of this investigation. These DOD levels are all located in the lower plateau with respect to voltage limits of this investigation. Different lithium polysulphides Li_2S_n $1 \leq n \leq 8$ exist in the second plateau [5]. The highest recovered capacity is expected at the highest DOD level because of the increasing concentration of precipitated Li_2S during the discharge process in the second plateau. So in every recovery cycle one DOD level is tested with one t_{RBT}.
The third parameter is the discharge current. Three varied discharge currents 0.2C, 0.4C and 0.8C were used to measure the recovered capacity. We assumed that the amount of recovered capacity increases at higher discharge currents because of the less homogeneous precipitated Li_2S structure.

3.4 Basic Recovery Model

The cell capacity is highly current dependent as shown in Fig.2 and as described in section 1 and 2. Part of the blocked capacity can be recovered. The recovered capacity is calculated using equation 4 by subtraction of the cumulated discharged capacity of the fourth cycle and the discharged capacity of the second cycle of the same cell (section 3.2). The recovery model is built using equation 4 and 5.

$$Q_{Rec} = Q_{4thCycle_{(t_{RBT}, i_{CRate}, DOD)}} - Q_{2ndCycle_{(i_{CRate})}} \tag{4}$$

The first recovery time constant investigation presented in section 3.1 motivated to model the recovery capacity by equation 5.

$$Q_{Rec} = ke^{-\frac{t_{RBT}}{\tau}} \tag{5}$$

4 Results

4.1 Constant current condition

This section focusses on the model and the results of the recovery capacity investigation. The gain factor k and the time constant τ as defined in equation 5 were estimated by least-squares method to build the model in the best possible quality. The estimated models are shown in Fig.4 dependent on gain factor and time constant. All recovered capacities in Fig.4 are normalized capacities by the nominal capacity at 0.2C constant discharge current.

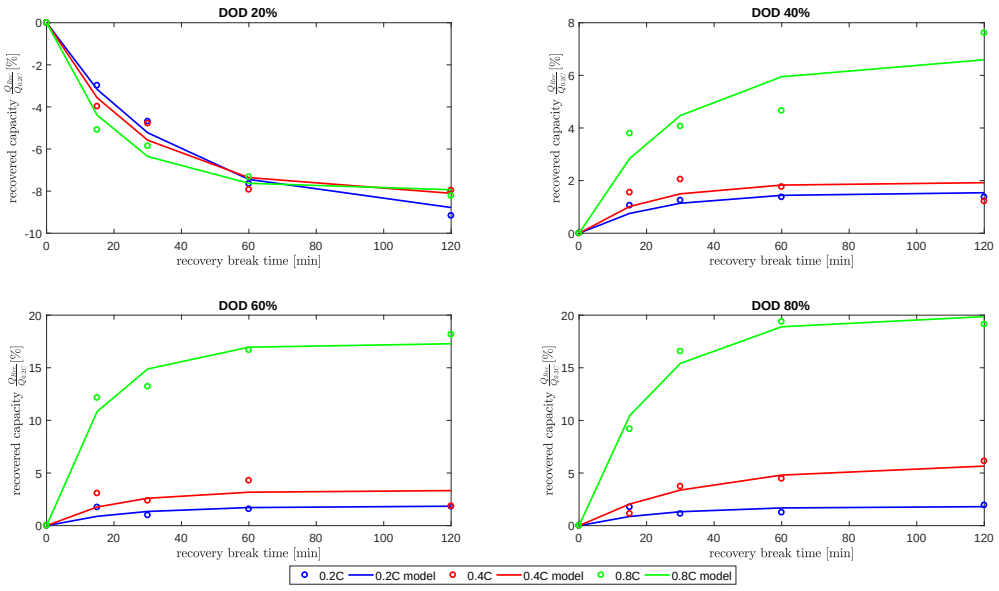

Figure 4: Model of the relative recovered cell capacities at 20%, 40%, 60%, 80% DOD level and discharge currents of 0.2C, 0.4C, 0.8C measured at a constant temperature of $25°C$.

At DOD 20% the measurements show a negative recovered capacity for every discharge current. At that DOD the cell capacity shows a high decrease about 8 to 9% at 120 min t_{RBT}. So an inclusion of t_{RBT} at a high DOD level decreases the discharged capacity compared to the same varied constant current discharge without t_{RBT}. The investigated 20% DOD level is already in the second plateau, with respect to voltage limits of this investigation as Fig.1 shows. In the second plateau at 20% DOD level, precipitated Li_2S exists in a low concentration [5]. Nevertheless, this small concentration of Li_2S don't block much active material which could be unblocked by the recovery effect during the t_{RBT}. In other words, the recovery effect doesn't explain the decreased discharged capacity. The cell temperature is considered next. It is well known that the cell temperature has a high influence on the discharge capacity in LiS cells. One reason for this influence is the high amount of electrolyte in LiS cells. The t_{RBT} forces the inner cell temperature to return to temperature equilibrium condition and reduces cell kinetics based on Arrhenius law. Consequently, these findings show contrary mechanisms between the recovered

capacity during the t_{RBT} and the decreasing inner cell temperature during the t_{RBT}. So the lower inner cell temperature reduces the discharged capacity more than capacity is recovered due to unblocked active materials. In other words the concentration of precipitated Li_2S is too small.
The results of all t_{RBT} at 40%, 60% and 80% DOD show an increasing amount of recovered capacity for all discharged current rates. The recoverable capacity increases with higher DOD levels due to the increase of Li_2S concentration and the diffusion of polysulfides to the active surface. So the recovered capacity dominates the contrary mechanism between the recovered capacity during the t_{RBT} and decreasing inner cell temperature during t_{RBT}. The recovered capacity due to the unblocked active material increases the discharge capacity more than the discharged capacity is reduced by lower inner cell temperature. As expected, the recovered capacity highly increases with higher DOD, with higher discharge current and with higher t_{RBT}. Up to 20% of the cell capacity is recovered due to the concentration of Li_2S and the amount of blocked active material.
The measurements for every DOD and discharge current are separate modelled by a first order differential equation which is solved in equation 5. The final recovery capacities of these separate models at $t_{RBT} = 120$ minutes are nonlinear related as we illustrate in Fig.5.

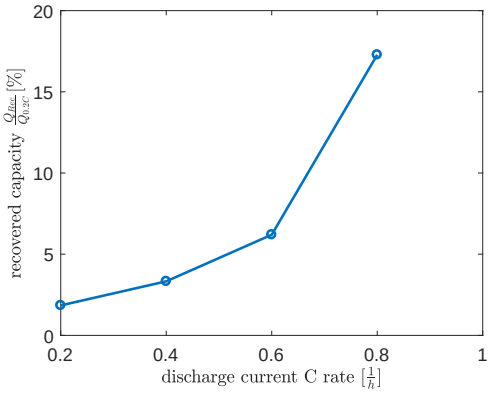

Figure 5: Measured recovered capacity for 120 minutes t_{RBT} at DOD 60% at 0.2C, 0.4C, 0.6C and 0.8C and at a constant temperature of $25°C$.

Furthermore, the result of Fig.4, and table 1 present a mean time constant $\bar{\tau}$ within the range of 17.9 and 24.4 minutes. This is in the same range as the published time constant in [8].

Table 1: Discharge current dependent mean time constant $\bar{\tau}$ of equation 5 measured at a constant temperature of $25°C$

	$I_{0.2C}$	$I_{0.4C}$	$I_{0.8C}$
$\bar{\tau}$	17.9	24.4	21.6

In order to quantify the modelled quality the root mean square of the recovery model for every discharge current and every DOD is shown in table 2. This shows that the highest error of the model is at 60% DOD. Good agreements are given for 20% and 80%.

Table 2: Root mean square error between measured and modelled recovered capacity, normalized by the nominal discharge capacity at 0.2C and measured at a constant temperature of $25°C$.

	20 % DOD	40 % DOD	60 % DOD	80 % DOD
0.2C discharge	0.04 %	0.01%	0.07%	0.08%
0.4C discharge	0.09 %	0.10%	0.42%	0.1 %
0.8C discharge	0.08 %	0.35%	0.48%	0.28%

In order to test the modelled capacity recovery effect, the same recovery cycle as described in section 3.2 was applied for a discharge current of 0.6C with a t_{RBT} of 120 minutes at 60% DOD. This investigation

intents to test the feasibility of the model interpolation between the measured discharge current of 0.4C and 0.8C. The measured recovered capacity in this recovery cycle was 6.2% (see Fig.5), whereas the modelled recovery capacity is 9.5% by interpolating the recovery model between 0.4C and 0.8C. If the modelled recovered capacity from 0.2C to 0.4C is extrapolated the modelled recovery capacity is 4.75% for this 0.6C investigation. These recovery capacities don't fit the measured ones for interpolation or extrapolation. So a linear interpolation of the recovered capacity at 0.4C of constant current investigation and at 0.8C of the first recovery time constant investigation in section 3.1 was used and showed that the measured recovered capacity of 0.6C is reasonable. Therefore, the gain of the first recovery time constant investigation was interpolated from 100% DOD to 60% DOD with respect to the DOD dependent gain results in our measurements in Fig.4. A recovery capacity of 5.6% was calculated by model interpolation. The measured recovered capacity of 6.2% at 0.6C is higher as our model predicts, but reasonable with respect to table 2.

4.2 Drive cycle condition

In this section time variant currents are investigated based on a drive cycle. Due to the fact that the recovery capacity is interesting for vehicular applications an drive cycle with a LiS traction battery was investigated. This LiS traction battery was downsized on cell level and measured in our lab.

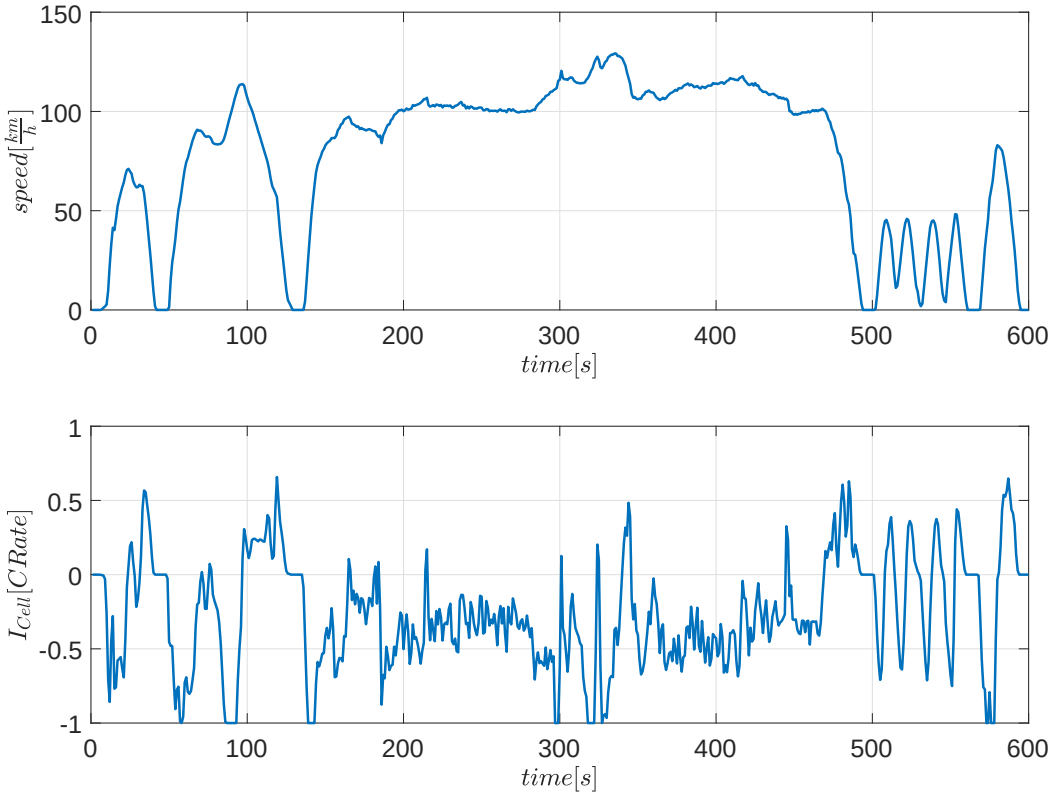

Figure 6: Velocity and calculated current profile of the US06 drive cycle. Discharged current is negative.

Today 68% of daily travel of light-duty vehicles is about 40 miles per day [15]. The electric vehicle journey time is short compared to rest time periods. In vehicular applications, these rest time periods have an important influence on the usable cell capacity and DOD in LiS batteries due to the recovery effect. Therefore the basic recovery model is tested at separate cells with two different time variant current profiles based on US06 drive cycle. This drive cycle was already used in [16] because of the high amount of recuperation parts. It shows a maximum possible real condition opposite to a recovery effect based on constant current discharge. The drive cycle and the used current profile are shown in Fig. 6. This US06 drive cycle was used to calculate current profiles for commercial LiS cells. The current profile as shown in Fig.6 was separately scaled to a maximum discharge current of 0.5C and 1C by a light-duty vehicle.

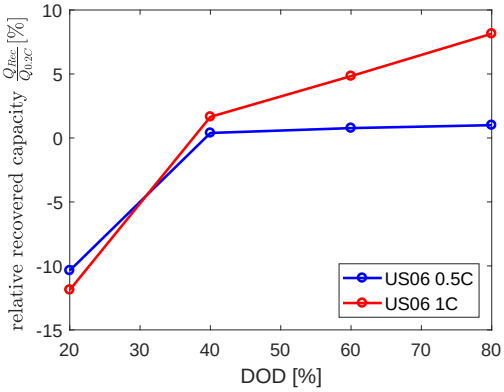

Figure 7: Relative recovered cell capacity by the US06 drive cycle for a maximum discharge current of 0.5C and 1C, measured at a constant temperature of $25°C$.

Each cell was discharged with repetitions of one of the two scaled current profiles of the US06 drive cycle. These repeated current profiles discharged the cell to the same DOD levels as described in section 3.3. At these DOD levels a t_{RBT} of 120 minutes was included in order to check the maximum recovered capacity. Afterwards the cell is further discharged at repeated current profiles of the scaled US06 current profile. The results presented in Fig.7, show the expected negative recovered capacity at 20% DOD. Beside this the results for the US06 1C at 60% and 80% DOD are unexpectedly high. At 80% DOD it shows a recovered capacity of 8%. The results of the scaled 0.5C US06 drive cycle fit to the US06 0.5C mean current of the current profile ($\bar{I}_{US060.5C}$=$-0.14A$), whereas the recovered capacities of the scaled 1C US06 drive cycle highly differ from the modelled recovered capacity by US06 1C mean current ($\bar{I}_{US061C}$=$-0.27A$). The modelled recovered capacity at a discharge current of $\bar{I}_{US061C}$ at 80% DOD is 3.2%. The calculated mean currents of the drive cycle consider each current $I_{US06(t)}$ by the same weight.

4.3 Discussion

Our study demonstrates a DOD and current dependent capacity recovery effect. Obviously the findings in the constant current investigation in section 4.1 show a first order differential equation behaviour for constant currents.
The recovery model calculates a to high recovered capacity for a 0.6C discharge current at 60% DOD. As section 4.1 shows a reasonable recovered capacity can be estimated with respect to the first recovery time constant investigation. This can be explained by assuming that the recovered capacity of the 0.8C model is too high. The findings of the recovered capacity for discharge current at 0.8C for 60% and for 80% DOD of up to 20% seem to be too high compared to the maximum of 10.5% recovered capacity of the first recovery time constant investigation in section 3.1. One explanation for the finding of this high recovered capacity might be an increasing age of the cell. The decreased discharge capacity of the cell at high currents is more influenced than at low currents. Compared to constant current discharge, the discharge with t_{RBT} at a higher aged state could recover some capacity and in addition might use dissolved non utilized polysulfides which diffuse back to the active surface. However, the normalized recovered capacity is in the same range as the normalized recovered capacity in [8] at 1C. In contrary to the results in [8] we couldn't recover the whole non utilized sulphur capacity. The difference in our study and the findings of [8] might also be that the t_{RBT} is included at 100% DOD in [8] and at a maximum 80% DOD in our study. A further explanation could be due to different cell designs. Further investigations on recovery effect and ageing have to be made.
Although there are some higher root mean square errors for data of 60% DOD in comparison to the root mean square errors of the other DODs (see table 2), they still seem reasonably compared to the amount of recovered capacity and to the other model errors.
Our data in table 1 confirms that τ at different DOD levels suit to the recovery time constant of 100% DOD published in [8]. Although they are very small at 0.2C.
Our additional results at drive cycle conditions offers evidence that the provided model cannot estimate recovered capacity of time variant currents due to current averaging before the t_{RBT}. The assumption of equally weighted current on the recovery effect is not feasible. The 1C US06 drive cycle provided a remarkable higher recovered capacity than estimated by current averaging. The difference between the actual recovered capacity and the estimated recovered capacity due to current averaging is probably due to the nonlinearity of the Li_2S blocking process by time variant currents. The constant current investigation provides little information about this blocking process due to time variant currents. It

seems that 0.5C US06 doesn't heavily influence the recovery effect due to time variant currents.
We readily acknowledge that this model is limited to constant current discharge profiles. We therefore recommend further investigations towards dynamic current discharge profiles. An alternative to the averaged current as input parameter for the recovery model might be the grade of blocked active material. However, the present study offers clear evidence that the recovery effect is an important mechanism to be considered in vehicular applications.

5 Conclusion

In our capacity recovery study, we have provided valuable results on the impact of recovery break time on usable capacity in LiS batteries at different DODs: We have shown that it is possible to build an applicable capacity recovery model with respect to DOD, discharge current and recovery break time. Moreover, the recovered capacity highly increases with increasing of every single one of these parameters.
Our study has shown that the highly current dependent LiS capacity can be recovered by a maximum amount of 20% of the nominal cell capacity at 0.8C and 80% DOD. However, the ageing of cells seems to influence the recovered capacity.
The investigation showed negative recovered capacities at 20% DOD for every recovery break time and discharge current due to a low concentration of precipitated Li_2S and reduction of inner cell temperature during the recovery break time. At this DOD more capacity is useable by reducing recovery break times. A positive capacity is recovered for 40% DOD and higher. This recovered capacity is increasing with DOD and discharge current until a maximum recovery break time of 120 minutes. The recovered capacity was modelled by a first order differential equation.
Although this investigation provides a basic recovery model, there are still open questions for further research on the recovery effect in LiS cells. The model calculated at constant current discharges couldn't estimate a drive cycle properly with time variant currents. The recovered capacity from the drive cycle and consequently from time variant currents was remarkably high. We therefore recommend that weighted time variant currents are used to properly estimate the capacity recovery in future researches.
Nevertheless, the investigation shows that the capacity recovery effect is an important effect to properly estimate the true usable capacity in LiS batteries for vehicular and other applications.

References

[1] S. Urbonaite et.al., *Progress Towards Commercially Viable Li-S Battery Cells*, Advanced Energy Materials, ISSN 1614-6840, 5(2015), n/a-n/a.

[2] *VDI*, https://www.vdi.de/, accessed on 2017-06-24.

[3] M. Barghamadi et al., *A Review on Li-S Batteries as a High Efficiency Rechargeable Lithium Battery*, Journal of The Electrochemical Society, 160(2013), 1256-1263.

[4] P. Busche et.al., *Systematical electrochemical study on the parasitic shuttle-effect in lithium-sulfur-cells at different temperatures and different rates*, Journal of Power Sources, ISSN 0378-7753, 259(2014), 289-299.

[5] V. Kolosnitsyn et al., *On the reasons for low sulphur utilization in the lithium-sulphur batteries*, Journal of Power Sources, ISSN 0378-7753, 274(2015), 203-210.

[6] Y. Mikhaylik et al., *Polysulfide Shuttle Study in the Li/S Battery System*, Journal of The Electrochemical Society, 151(2004), 1969-1976.

[7] S.Waluś et al., *Lithium/sulfur Batteries Upon Cycling: Structural Modifications and Species Quantification by In Situ and Operando X-Ray Diffraction Spectroscopy*, Advanced Energy Materials, ISSN 1614-6840, 27(2015), 5203-5209

[8] T. Zhang et al., *Modelling transport-limited discharge capacity of lithium-sulfur cells*, Electrochimica Acta, ISSN 0013-4686, 219(2016), 502-508.

[9] C. Parfitt, *Characterisation, Modelling and Management of Lithium-Sulphur Batteries for Spacecraft Applications*, Dissertation, University of Warwick, 2012.

[10] V. Knap et al., *Electrical circuit models for performance modeling of Lithium-Sulfur batteries*, Energy Conversion Congress and Exposition (ECCE), Montreal, 2015.

[11] K. Kumaresan et al., *A Mathematical Model for a Lithium-Sulfur Cell*, Journal of The Electrochemical Society 155(2008) A576-A582,

[12] M. Marinescu et al., *A zero dimensional model of lithium-sulfur batteries during charge and discharge*, Physical Chemistry Chemical Physics, ISSN 1463-9084, 18(2015), 584-593.

[13] S. Zhang et al., *Liquid electrolyte lithium/sulfur battery: Fundamental chemistry, problems, and solutions*, Journal of Power Sources, ISSN 0378-7753, 231(2013), 153-162.

[14] K. Hancock et al., *Electrolyte decomposition in Li-S cells*, Li-SM3 Conference, London, England, 2017.

[15] D.Howell, *Update on US DOE Electric Drive Vehicle R&D and Deployment Activities*, 6th US-China Electric Vehicle and Battery Technology Workshop, Massachusetts, USA, 2012.

[16] P. Keil et al., *Aging of Lithium-Ion Batteries in Electric Vehicles: Impact of Regenerative Braking*, 28th EVS, Goyang, Korea, 2015.

Authors

M. Sc. Christian Maurer earned his master's degree in electrical engineering from the University of Applied Sciences Darmstadt in 2014. Currently, he is working as research associate at the Institute of Automotive Technologies at the University of Applied Sciences in Ulm. His main reasearch activities are in the field of modelling and characterization of Li-S cells.

Prof. Dr. Walter Commerell holds a professorship at the University of Applied Sciences Ulm. His research areas at the Institute of Energy- and Drive Technologies are energy storages in stationary and mobile applications as well as energy management in different systems.

Prof. Dr. Dr. med. Andreas Hintennach is a chemist and medical doctor. He received his PhD in electrochemistry from the ETH Zurich and Paul Scherrer Institute (Switzerland) in 2010. After a postdoc stay at MIT 2010-11 he joined the research department of Mercedes-Benz. His present focus in the field of electrochemistry is fundamental research on next generation electrical energy storage and conversion materials and systems, sustainability and toxicology.

Prof. Dr.-Ing. Andreas Jossen holds a professorship at the Technical University Munich and he is the founder and head of the Institute of Electrical Energy Storage Technology. His research activities are modeling, simulation, and characterization of rechargeable batteries and fundamental and applied topics in battery systems, such as battery topologies, state determination, and control of battery systems.